Research Article

International Journal of Distributed Sensor Networks

International Journal of Distributed Sensor Networks
2021, Vol. 17(2)

DOI: 10.1177/15501477721991770
journals.sagepub.com/home/dsn
SAGE

Interval analysis-based Bi-iterative algorithm for robust TDOA-FDOA moving source localisation

Ningning Qin[1,2], Chao Wang[1], Changxu Shan[1] and Le Yang[3]

Abstract

In this study, an interval extension method of a bi-iterative is proposed to determine a moving source. This method is developed by utilising the time difference of arrival and frequency difference of arrival measurements of a signals received from several receivers. Unlike the standard Gaussian noise model, the time difference of arrival - frequency difference of arrival measurements are obtained by interval enclosing, which avoids convergence and initialisation problems in the conventional Taylor-series method. Using the bi-iterative strategy, the algorithm can alternately calculate the position and velocity of the moving source in interval vector form. Simulation results indicate that the proposed scheme significantly outperforms other methods, and approaches the Cramer-Rao lower bound at a sufficiently high noise level before the threshold effect occurs. Moreover, the interval widths of the results provide the confidence degree of the estimate.

Keywords

Time difference of arrival (TDOA), frequency difference of arrival (FDOA), bi-iterative, intervals enclosing, Taylor-series method

Date received: 10 January 2020; accepted: 5 January 2021

Handling Editor: Lyudmila Mihaylova

Introduction

Passive source localisation based on time difference of arrival (TDOA) and frequency difference of arrival (FDOA) measurements has become a topic of interest owing to its wide application in radar,[1] navigation,[2] interference localisation,[3] and wireless networks.[4] For the high nonlinearity implied in the measurement equations, many available methods for solving TDOA- and FDOA-based moving source localisation have been proposed. The traditional method in Foy,[5] and Lu and Ho[6] linearises the equations via Taylor-series expansion. Two drawbacks must also be considered. First, an initial solution is required to obtain the source estimate. Second, the convergence is not guaranteed. To avoid these issues, researchers have investigated algebraic methods, which allow the independence of the initial estimate and have high computationally efficient.[7] Among these methods, the two-step weight least-square (TSWLS) method,[8,9] is popular, and can provide an algebraic solution without an initial guess. Interestingly, the closed-form result of the TSWLS reaches the Cramer-Rao lower bound (CRLB) at the low-noise level. However, it shows poor localisation accuracy when the target approaches the axis of the

[1]Key Laboratory of Advanced Process Control for Light Industry of Ministry of Education, Jiangnan University, Wuxi, China
[2]Key Laboratory of Dynamic Cognitive System of Electromagnetic Spectrum Space, Ministry of Industry and Information Technology, Nanjing University of Aeronautics and Astronautics, Nanjing, China
[3]The Department of Electrical and Computer Engineering Department, University of Canterbury, Christchurch, New Zealand

Corresponding author:
Ningning Qin, Key Laboratory of Advanced Process Control for Light Industry of Ministry of Education, Jiangnan University, Wuxi 214122, Jiangsu, China.
Email: ningning801108@163.com

reference sensor. The method discussed in, Zou and Liu[10] and Zhou, et al.[11] is proposed to transform the maximum likelihood estimator problem into a convex optimisation problem, but its results are more robust at high computational complexity. The CTLS algorithm[12] overcomes the problem that the total least squares algorithm cannot achieve the optimal solution when the noise components are statistically correlated, and can achieve CRLB when the measurement noise is moderate. However, due to the influence of the target and the location distribution of the external radiation source, the coefficient matrix may have ill-conditioned problems, resulting in huge fluctuations in the results of the equation solution due to small observation errors, and degrading the performance of the CTLS algorithm. The bi-iterative technique recently proposed in, Zhu and Feng[13] and Zhu et al.[14] can reduce the computational cost by alternately calculating the source location and velocity. The mentioned methods assume that the TDOA and FDOA noises both accord with the Gaussian distribution. They only provide the point estimates of the source position and velocity, and not a confidence interval.

From the Taylor-series expansion, this work derives the interval extension of the bi-iterative method for a moving source localisation based on the bounded error framework. The proposed algorithm combines the interval analysis technique in, Abdallah et al.,[15] and Jaulin and Walter[16] with a bi-iterative strategy[13,14] to estimate the target position and velocity. Compared to the traditional iterative method, the novel scheme obtains estimations of the source in interval vector form, which has a 95% probability[17] of containing the true vales. It allows global convergence and avoids the initialisation problem. Furthermore, the interval widths of the results provide the estimated confidence.

The rest of this paper is organised as follows: Section 2 defines the symbols and notations. Section 3 discusses the measurement model. The details of the interval analysis-based bi-iterative algorithm are shown in Section 4. Section 5 deduces the CRLB and the mean square error (MSE) of the source location and velocity estimates. Section 6 provides the simulation results, and valuable conclusions are presented in Section 7.

Symbols and notations

We denote the punctual column vectors and matrices in bold lower and upper-case letters, respectively. For $n \times 1$ vector $\boldsymbol{x}$, x_i, $i = 1, 2, ..., n$, represents the ith component. For $n \times m$ matrix $\boldsymbol{A}$, $A_{i,j}$ is the entry in the ith row and jth column, where $i = 1, 2, ..., n$ and $j = 1, 2, ..., m$.

In the interval number system, $[x]$ denotes the closed set $[\underline{x}, \bar{x}] = \{x \in \mathbf{R}, \underline{x} < x < \bar{x}\}$ and is referred to as an interval scalar $[*]$. $\underline{x}$ and $\bar{x}$ are called the lower and upper endpoints of $[x]$, respectively. If $\underline{x} = \bar{x}$, then $[x]$ degenerates to a scalar (i.e. in this case, $[x] = \bar{x}$). The midpoint of $[x]$ is equal to $mid([x]) = \frac{1}{2}(\underline{x} + \bar{x})$, and its width is defined as $w([x]) = \bar{x} - \underline{x}$.

To operate on the interval, we extend the basic calculation of the floating-point numbers and the set operations, such as $+$, $-$, $*$, $\div$, $\cap$ and $\cup$, into the interval analysis.[18] The interval correspondence of functions is usually impossible to calculate. Thus, the concept of inclusion function is proposed. The inclusion function $[f](\cdot)$ for a function $f(\cdot)$ indicates that the image of interval $[x]$ by $[f](\cdot)$ is an interval containing $f([x])$.[19]

Measurements model

We consider a scenario of M ($M > 4$) moving or stationary sensors that collaborate to determine a moving target with an unknown position $\boldsymbol{u} = [x, y, z]^T$ and velocity $\dot{\boldsymbol{u}} = [\dot{x}, \dot{y}, \dot{z}]^T$ using TDOA and FDOA measurements in three dimensional space. Sensor position $\boldsymbol{s}_i = [x_i, y_i, z_i]^T$ and velocity $\dot{\boldsymbol{s}}_i = [\dot{x}_i, \dot{y}_i, \dot{z}_i]^T$, $i = 1, 2, ..., M$, are accurately derived by an estimator. Without loss of generality, the first sensor is set as the reference.

The accurate TDOA measurement between sensor pair i ($i = 1, 2, ..., M$) and 1 multiplied by the speed of propagation, known as the range difference of arrival, is

$$d_{i,1} = d_i - d_1 = \Delta\tau_{i,1} c \tag{1}$$

where

$$d_i = \|\boldsymbol{u} - \boldsymbol{s}_i\| \tag{2}$$

is the distance from the target to the ith sensor, and c is the signal propagation speed.

Similarly, the FDOA measurement between sensor i ($i = 1, 2, ..., M$) and the reference sensor multiplied by the speed of propagation is

$$\dot{d}_{i,1} = \dot{d}_i - \dot{d}_1 = \frac{\Delta f_{i,1}}{f_0} c \tag{3}$$

where

$$\dot{d}_i = \frac{(\boldsymbol{u} - \boldsymbol{s}_i)^T (\dot{\boldsymbol{u}} - \dot{\boldsymbol{s}}_i)}{\|\boldsymbol{u} - \boldsymbol{s}_i\|} \tag{4}$$

is the time derivative of (2), and f_0 is the carrier frequency.

Through the combination of equations (1) and (3), the TDOA and FDOA measurements are modelled as

$$d^o_{i,1} = d_{i,1} + \Delta d_{i,1} \tag{5a}$$

$$\dot{d}^o_{i,1} = \dot{d}_{i,1} + \Delta \dot{d}_{i,1} \tag{5b}$$

where $\Delta d_{i,1}$ and $\Delta \dot{d}_{i,1}$ are the measurement noises of TDOA and FDOA, respectively. The TDOA and FDOA measurements can be arranged into two $M-1$ column vectors

$$\boldsymbol{d}^o = [d^o_{2,1}, ..., d^o_{M,1}]^T = \boldsymbol{d} + \Delta\boldsymbol{d} \tag{6a}$$

$$\dot{\boldsymbol{d}}^o = [\dot{d}^o_{2,1}, ..., \dot{d}^o_{M,1}]^T = \dot{\boldsymbol{d}} + \Delta\dot{\boldsymbol{d}} \tag{6b}$$

where $\boldsymbol{d} = [d_{2,1}, ..., d_{M,1}]^T$ and $\dot{\boldsymbol{d}} = [\dot{d}_{2,1}, ..., \dot{d}_{M,1}]^T$. The corresponding noise vectors $\Delta\boldsymbol{d} = [\Delta d_{2,1}, ..., \Delta d_{M,1}]^T$ and $\Delta\dot{\boldsymbol{d}} = [\Delta\dot{d}_{2,1}, ..., \Delta\dot{d}_{M,1}]^T$.

To simplifying the noise error calculation, equation (6a) and (6b) can be transformed into the interval forms in accordance with the 3-sigma principle.[17] The updated equations can be obtained as

$$\boldsymbol{d}^o \in [\boldsymbol{d}^o] = [[d^o_{2,1}], ..., [d^o_{M,1}]]^T = \boldsymbol{d} + [\Delta\boldsymbol{d}] \tag{7a}$$

$$\dot{\boldsymbol{d}}^o \in [\dot{\boldsymbol{d}}^o] = [[\dot{d}^o_{2,1}], ..., [\dot{d}^o_{M,1}]]^T = \dot{\boldsymbol{d}} + [\Delta\dot{\boldsymbol{d}}] \tag{7b}$$

where $[\Delta\boldsymbol{d}] = [[\Delta d_{2,1}], ..., [\Delta d_{M,1}]]^T$ and $[\Delta\dot{\boldsymbol{d}}] = [[\Delta\dot{d}_{2,1}], ..., [\Delta\dot{d}_{M,1}]]^T$ are the error boundaries of TDOA and FDOA respectively; $[d^o_{i,1}] = \{d_{i,1} - 3\delta_{i,1} \leq d^o_{i,1} \leq d_{i,1} + 3\delta_{i,1}\}$ and $[\dot{d}^o_{i,1}] = \{\dot{d}_{i,1} - 3\dot{\delta}_{i,1} \leq \dot{d}^o_{i,1} \leq \dot{d}_{i,1} + 3\dot{\delta}_{i,1}\}, i = 1, 2, ..., M$ are the TDOA and FDOA interval measurements, where $\delta_{i,1}$ and $\dot{\delta}_{i,1}$ are the noise variances of TDOA and FDOA, respectively. For notation simplicity, we have $[\boldsymbol{d}^o]$ and $[\dot{\boldsymbol{d}}^o]$ in interval vector $[\boldsymbol{m}^o] = [[\boldsymbol{d}^o]^T, [\dot{\boldsymbol{d}}^o]^T]^T$. The true TDOA and FDOA measurements vector is $\boldsymbol{m}^o = [\boldsymbol{d}^{oT}, \dot{\boldsymbol{d}}^{oT}]^T \in [\boldsymbol{m}^o]$.

Localisation algorithm

Let $\theta = [\boldsymbol{u}^T, \dot{\boldsymbol{u}}^T]^T$ be the unknown parameter of the true location and velocity of the moving source, using TDOA-FDOA measurements to estimate θ that can be expressed as

$$\Delta\boldsymbol{m} = \boldsymbol{m}^o - \boldsymbol{m}_{(\theta)} \tag{8}$$

where $\Delta\boldsymbol{m} = [\Delta\boldsymbol{d}^T, \Delta\dot{\boldsymbol{d}}^T]^T$ is an approximately zero-mean Gaussian noise and its covariance matrix is

$$\boldsymbol{Q} = \begin{bmatrix} \boldsymbol{Q}_{\boldsymbol{d}} & 0_{(M-1)\times(M-1)} \\ 0_{(M-1)\times(M-1)} & \boldsymbol{Q}_{\dot{\boldsymbol{d}}} \end{bmatrix} \tag{9}$$

where $\boldsymbol{Q}_{\boldsymbol{d}}$ is the covariance matrix for TDOA measurement noise and $\boldsymbol{Q}_{\dot{\boldsymbol{d}}}$ is the covariance matrix for FDOA measurement noise. Noise vectors $\Delta\boldsymbol{d}$ and $\Delta\dot{\boldsymbol{d}}$ are assumed to be independent with one another. Original interval vectors $[\boldsymbol{u}]$ and $[\dot{\boldsymbol{u}}]$ can be obtained from prior knowledge, such as the sensors' coverage area and the maximum source speed. Based on the relationship of the TDOA-FDOA measurements in equations (1) and (4), we can redefine $\boldsymbol{m}_{(\theta)} = [\boldsymbol{d}^T_{(\theta)}, \dot{\boldsymbol{d}}^T_{(\theta)}]^T$, where $\boldsymbol{d}_{(\theta)} = [d_{2,1}, ..., d_{M,1}]$ and $\dot{\boldsymbol{d}}_{(\theta)} = [\dot{d}_{2,1}, ..., \dot{d}_{M,1}]$.

First, we consider the situation where the target velocity $\dot{\boldsymbol{u}}_{1m} = \text{mid}([\dot{\boldsymbol{u}}])$ is fixed. If $\boldsymbol{u}_m = \text{mid}([\boldsymbol{u}])$ is assumed as the initial position solution, equation (8) can be solved by the Taylor-series expansion of $\boldsymbol{m}_{(\theta)}$ around $\boldsymbol{u}_m$ as shown in

$$\boldsymbol{m}^o - \Delta\boldsymbol{m} \approx \tilde{\boldsymbol{m}} - \boldsymbol{J}_1(\boldsymbol{u} - \boldsymbol{u}_m) \tag{10}$$

where $\tilde{\boldsymbol{m}} = [\tilde{\boldsymbol{d}}^T, \dot{\tilde{\boldsymbol{d}}}^T]^T$, $\tilde{\boldsymbol{d}} = [\tilde{d}_{2,1}, ..., \tilde{d}_{M,1}]$ and $\dot{\tilde{\boldsymbol{d}}} = [\dot{\tilde{d}}_{2,1}, ..., \dot{\tilde{d}}_{M,1}]$. And there are

$$\tilde{d}_{i,1} = \|\boldsymbol{u}_m - \boldsymbol{s}_i\| - \|\boldsymbol{u}_m - \boldsymbol{s}_1\| \tag{11a}$$

$$\dot{\tilde{d}}_{i,1} = \frac{(\boldsymbol{u}_m - \boldsymbol{s}_i)^T(\dot{\boldsymbol{u}}_{1m} - \dot{\boldsymbol{s}}_i)}{\|\boldsymbol{u}_m - \boldsymbol{s}_i\|} - \frac{(\boldsymbol{u}_m - \boldsymbol{s}_1)^T(\dot{\boldsymbol{u}}_{1m} - \dot{\boldsymbol{s}}_1)}{\|\boldsymbol{u}_m - \boldsymbol{s}_1\|} \tag{11b}$$

In addition, Jacobian matrix $\boldsymbol{J}_1$ is shown in

$$\boldsymbol{J}_1 = \left(\frac{\partial \boldsymbol{m}_{(\theta)}}{\partial \boldsymbol{u}}\right)\Big|_{\boldsymbol{u}=\boldsymbol{u}_m} \tag{12}$$

and the derivation of partial derivative $\left(\frac{\partial \boldsymbol{m}_{(\theta)}}{\partial \boldsymbol{u}}\right)$ is shown in

$$\frac{\partial \boldsymbol{m}_{(\theta)}}{\partial \boldsymbol{u}} = \begin{bmatrix} \frac{\partial \boldsymbol{d}}{\partial \boldsymbol{u}} \\ \frac{\partial \dot{\boldsymbol{d}}}{\partial \boldsymbol{u}} \end{bmatrix} \tag{13}$$

where the (i-1)th rows of $(\partial\boldsymbol{d}/\partial\boldsymbol{u})$ and $(\partial\dot{\boldsymbol{d}}/\partial\boldsymbol{u})$ are given by, $i = 2, ..., M$

$$\frac{\partial \boldsymbol{d}}{\partial \boldsymbol{u}}(i-1, :) = \frac{(\boldsymbol{u} - \boldsymbol{s}_i)^T}{d_i} - \frac{(\boldsymbol{u} - \boldsymbol{s}_1)^T}{d_1} \tag{14a}$$

$$\frac{\partial \dot{\boldsymbol{d}}}{\partial \boldsymbol{u}}(i-1, :) = \frac{\dot{d}_1(\boldsymbol{u} - \boldsymbol{s}_1)^T}{d_1^2} - \frac{\dot{d}_i(\boldsymbol{u} - \boldsymbol{s}_i)^T}{d_i^2} \tag{14b}$$

In accordance with equation (10), the least square (LS) estimator of $\boldsymbol{u}$ is shown in

$$\boldsymbol{u} = \boldsymbol{u}_m - (\boldsymbol{J}_1^T\boldsymbol{Q}_r^{-1}\boldsymbol{J}_1)^{-1}\boldsymbol{J}_1^T\boldsymbol{Q}_r^{-1}(\boldsymbol{m}^o - \tilde{\boldsymbol{m}}) \tag{15}$$

where $\boldsymbol{Q}_r$ is the covariance matrix for TDOA measurement noise.

Given that $\boldsymbol{m}^o \in [\boldsymbol{m}^o]$ and $\tilde{\boldsymbol{m}} \in [\tilde{\boldsymbol{m}}]$, $[\boldsymbol{m}^o]$ and $[\tilde{\boldsymbol{m}}]$ are used instead of $\boldsymbol{m}^o$ and $[\tilde{\boldsymbol{m}}]$ in (15), we obtain

$$\boldsymbol{u} \in [\boldsymbol{u}] = \boldsymbol{u}_m - ([\boldsymbol{J}_1]^T\boldsymbol{Q}_r^{-1}[\boldsymbol{J}_1])^{-1}[\boldsymbol{J}_1]^T\boldsymbol{Q}_r^{-1}([\boldsymbol{m}^o] - [\tilde{\boldsymbol{m}}]) \tag{16}$$

The inverse of $([\boldsymbol{J}_1]^T\boldsymbol{Q}_r^{-1}[\boldsymbol{J}_1])$ is required to solve equation (16), which increases the computational cost. As for the nonlinearity implied in interval analysis, the idea of a midpoint test is proposed in Jaulin and Walter.[18] Essentially, reducing the computational complexity is effective.

Therefore, we simplify $[\boldsymbol{J}_1]$ with $\boldsymbol{J}_{1,m} = \mathrm{mid}([\boldsymbol{J}_1])$ in the case of lower location errors. The source position interval vector $[\boldsymbol{u}]$ can be solved using the following equation

$$[\boldsymbol{u}] \approx \boldsymbol{u}_m - (\boldsymbol{J}_{1,m}^T \boldsymbol{Q}_r^{-1} \boldsymbol{J}_{1,m})^{-1} \boldsymbol{J}_{1,m}^T \boldsymbol{Q}_r^{-1}([\boldsymbol{m}^o] - [\breve{\boldsymbol{m}}]) \quad (17)$$

Second, we consider another situation where source position $\boldsymbol{u}_{2m} = \mathrm{mid}([\boldsymbol{u}])$ is fixed, $[\boldsymbol{u}]$ is updated by equation (17), and $\boldsymbol{m}_{(\theta)}$ is expanded around $\dot{\boldsymbol{u}}_m = \mathrm{mid}([\dot{\boldsymbol{u}}])$, as shown in

$$\boldsymbol{m}^o - \Delta\boldsymbol{m} \approx \breve{\boldsymbol{m}} - \boldsymbol{J}_1(\dot{\boldsymbol{u}} - \dot{\boldsymbol{u}}_m) \quad (18)$$

$\breve{\boldsymbol{m}}$ and $\tilde{\boldsymbol{m}}$ are provided with the same functional form, where $\breve{\boldsymbol{m}} = [\breve{\boldsymbol{d}}\,T, \dot{\breve{\boldsymbol{d}}}^T]^T$, $\breve{\boldsymbol{d}} = [\breve{d}_{2,1}, ..., \breve{d}_{M,1}]$ and $\dot{\breve{\boldsymbol{d}}} = [\dot{\breve{d}}_{2,1}, ..., \dot{\breve{d}}_{M,1}]$. There are

$$\dot{\breve{d}}_{i,1} = \|\boldsymbol{u}_{2m} - \boldsymbol{s}_i\| - \|\boldsymbol{u}_{2m} - \boldsymbol{s}_1\| \quad (19a)$$

$$\dot{\breve{d}}_{i,1} = \frac{(\boldsymbol{u}_{2m} - \boldsymbol{s}_i)^T(\dot{\boldsymbol{u}}_m - \dot{\boldsymbol{s}}_i)}{\|\boldsymbol{u}_{2m} - \boldsymbol{s}_i\|} - \frac{(\boldsymbol{u}_{2m} - \boldsymbol{s}_1)^T(\dot{\boldsymbol{u}}_m - \dot{\boldsymbol{s}}_1)}{\|\boldsymbol{u}_{2m} - \boldsymbol{s}_1\|} \quad (19b)$$

Jacobian matrix $\boldsymbol{J}_2$ is shown in

$$\boldsymbol{J}_2 = \left(\frac{\partial \boldsymbol{m}_{(\theta)}}{\partial \dot{\boldsymbol{u}}}\right)\Big|_{\boldsymbol{u} = \dot{\boldsymbol{u}}_m} \quad (20)$$

and partial derivative $\left(\frac{\partial \boldsymbol{m}_{(\theta)}}{\partial \dot{\boldsymbol{u}}}\right)$ is shown in

$$\frac{\partial \boldsymbol{m}_{(\theta)}}{\partial \dot{\boldsymbol{u}}} = \begin{bmatrix} \frac{\partial \breve{\boldsymbol{d}}}{\partial \dot{\boldsymbol{u}}} \\ \frac{\partial \dot{\breve{\boldsymbol{d}}}}{\partial \dot{\boldsymbol{u}}} \end{bmatrix} \quad (21)$$

where

$$\frac{\partial \breve{\boldsymbol{d}}}{\partial \dot{\boldsymbol{u}}} = 0_{(M-1)\times 3} \quad (22a)$$

$$\frac{\partial \dot{\breve{\boldsymbol{d}}}}{\partial \dot{\boldsymbol{u}}} = \frac{\partial \breve{\boldsymbol{d}}}{\partial \boldsymbol{u}} \quad (22b)$$

According to equation (18), we can obtain the LS estimator of the source velocity, as shown in

$$\dot{\boldsymbol{u}} = \dot{\boldsymbol{u}}_m - (\boldsymbol{J}_2^T \boldsymbol{Q}_{\dot{r}}^{-1} \boldsymbol{J}_2)^{-1} \boldsymbol{J}_2^T \boldsymbol{Q}_{\dot{r}}^{-1}(\boldsymbol{m}^o - \breve{\boldsymbol{m}}) \quad (23)$$

where $\boldsymbol{Q}_{\dot{r}}$ is the covariance matrix for FDOA measurement noise.

Similar to the solution process of $[\boldsymbol{u}]$, $\boldsymbol{m}^o$ is first replaced with $[\boldsymbol{m}^o]$ in equation (23) to obtain the following formula

$$\dot{\boldsymbol{u}} \in [\dot{\boldsymbol{u}}] = \dot{\boldsymbol{u}}_m - ([\boldsymbol{J}_2]^T \boldsymbol{Q}_{\dot{r}}^{-1}[\boldsymbol{J}_2])^{-1}[\boldsymbol{J}_2]^T \boldsymbol{Q}_{\dot{r}}^{-1}([\boldsymbol{m}^o] - [\breve{\boldsymbol{m}}]) \quad (24)$$

Then, $\boldsymbol{J}_{2,m} = \mathrm{mid}([\boldsymbol{J}_2])$ is used to approximate $[\boldsymbol{J}_2]$ in equation (24), and $[\dot{\boldsymbol{u}}]$ can be obtained, as shown in

$$[\dot{\boldsymbol{u}}] \approx \dot{\boldsymbol{u}}_m - (\boldsymbol{J}_{2,m}^T \boldsymbol{Q}_{\dot{r}}^{-1} \boldsymbol{J}_{2,m})^{-1} \boldsymbol{J}_{2,m}^T \boldsymbol{Q}_{\dot{r}}^{-1}([\boldsymbol{m}^o] - [\breve{\boldsymbol{m}}]) \quad (25)$$

On the basis of the above description, $[\boldsymbol{u}]$ and $[\dot{\boldsymbol{u}}]$ can be alternately substituted in equations (17) and (25). Repeating the two steps can guarantee the convergence of the proposed algorithm because of the convergence of the Taylor-series algorithm near the solution. Moreover, instead of estimating the target position and velocity simultaneously, the developed method can alternately calculates the target position and velocity, which can simplify the derivative $\frac{\partial \boldsymbol{m}_{(\theta)}}{\partial [\boldsymbol{u}, \dot{\boldsymbol{u}}]}$ about the source position $\boldsymbol{u}$ and velocity $\dot{\boldsymbol{u}}$. The reduction of matrix dimension also can simplify the inverse process of derivative matrix about $\boldsymbol{m}_{(\theta)}$, and greatly reduces the computational cost. The midpoints of $[\boldsymbol{u}]$ and $[\dot{\boldsymbol{u}}]$ provide the point estimates of position and velocity for the source under small noise condition.

CRLB and performance analysis

CRLB

CRLB is the boundary of the unbiased estimation of variance. The results in this section are valid if the measurement noises are Gaussian, and their covariance matrices are known. Based on equation (6a) and (6b), the CRLB of the moving source localisation problem equals the inverse of the Fisher information matrix (FIM),[20] as shown in

$$CRLB = (\boldsymbol{J}^T \boldsymbol{Q}^{-1} \boldsymbol{J})^{-1} \quad (26)$$

where the Jacobian matrix $\boldsymbol{J}$ is shown in

$$\boldsymbol{J} = \left(\frac{\partial \boldsymbol{m}_{(\theta)}}{\partial [\boldsymbol{u}^T, \dot{\boldsymbol{u}}^T]^T}\right) \quad (27)$$

and the derivation of the partial derivative $\left(\left(\frac{\partial \boldsymbol{m}_{(\theta)}}{\partial [\boldsymbol{u}^T, \dot{\boldsymbol{u}}^T]^T}\right)\right)$ is shown in

$$\frac{\partial \boldsymbol{m}_{(\theta)}}{\partial [\boldsymbol{u}^T, \dot{\boldsymbol{u}}^T]^T} = \begin{bmatrix} \frac{\partial \breve{\boldsymbol{d}}}{\partial \boldsymbol{u}} & \frac{\partial \dot{\breve{\boldsymbol{d}}}}{\partial \boldsymbol{u}} \\ \frac{\partial \breve{\boldsymbol{d}}}{\partial \dot{\boldsymbol{u}}} & \frac{\partial \dot{\breve{\boldsymbol{d}}}}{\partial \dot{\boldsymbol{u}}} \end{bmatrix} \quad (28)$$

Thus, the position estimation accuracy of the proposed method is nearly identical to the CRLB under low noise conditions.

Performance analysis

In this subsection, we deduce the MSE of the source location and velocity estimates through the Taylor-series method at low TDOA and FDOA measurement

Table 1. The position (in metres) and velocities (in metres/second) of the sensors.

Sensor no.i	x_j	y_j	z_j	$\dot{x}_j$	$\dot{y}_j$	$\dot{z}_j$
1	300	100	150	30	−20	20
2	400	150	100	−30	10	20
3	300	500	200	10	−2	10
4	350	200	100	10	20	30
5	−100	−100	−100	−20	10	10

noise levels. If the iteration procedure in the localisation algorithm is terminated, then we can obtain the one-order Taylor-series expansion[21] at approximately $\theta = [\boldsymbol{u}^T, \dot{\boldsymbol{u}}^T]^T$ by combing equations (17) and (25). The equation can be obtained as shown in

$$\theta \approx \theta_m - (\boldsymbol{J}_m^T \boldsymbol{Q}^{-1} \boldsymbol{J}_m)^{-1} \boldsymbol{J}_m^T \boldsymbol{Q}^{-1} \Delta \boldsymbol{m} \tag{29}$$

where $\theta_m = [\boldsymbol{u}_m^T, \dot{\boldsymbol{u}}_m^T]^T$ is the final midpoint of position interval vector $[\boldsymbol{u}]$ and velocity interval vector $[\dot{\boldsymbol{u}}]$, and $\boldsymbol{J}_m = [\boldsymbol{J}_{1,m}, \boldsymbol{J}_{2,m}]$ is the approximate values of $[\boldsymbol{J}_1]$ and $[\boldsymbol{J}_2]$ under low noise conditions. Let $\Delta\theta = \theta - \theta_m$ denote the estimation errors of the source position and velocity, which is a zero-mean random vector.[22] Equation (29) can be transformed into

$$\Delta\theta = (\boldsymbol{J}_m^T \boldsymbol{Q}^{-1} \boldsymbol{J}_m)^{-1} \boldsymbol{J}_m^T \boldsymbol{Q}^{-1} \Delta \boldsymbol{m} \tag{30}$$

The covariance matrix of $\Delta\theta$ can be approximated by

$$cov(\Delta\theta) = E(\Delta\theta^T \Delta\theta) = (\boldsymbol{J}_m^T \boldsymbol{Q}^{-1} \boldsymbol{J}_m)^{-1} \tag{31}$$

Thus, the position and velocity estimation accuracy of the proposed method is nearly identical to the CRLB under low noise conditions. When the noise increases, the developed algorithm cannot guarantee the high accuracy of position and velocity estimation results, but the interval results can still estimate the range of the target position and velocity. Therefore, the proposed method provides anther idea for target localisation in high noise conditions.

Simulation

In this section, a set of Monte Carlo simulations evaluate the performance of the proposed algorithm by comparing it with TSWLS [8] and the maximum likelihood (ML) estimator[23] and CTLS.[12]

The localisation accuracy is evaluated in terms of the root mean square error (RMSE) and bias of the source location and velocity. The estimation bias in terms of the norm of estimation bias is defined as $bias(\boldsymbol{u}) = \left\| \frac{\sum_{n=1}^{N} \boldsymbol{u}_n}{N} - \boldsymbol{u} \right\|$ for the position and $bias(\dot{\boldsymbol{u}}) = \left\| \frac{\sum_{n=1}^{N} \dot{\boldsymbol{u}}_n}{N} - \dot{\boldsymbol{u}} \right\|$ for the velocity, where $\boldsymbol{u}_n$ and $\dot{\boldsymbol{u}}_n$ denote the estimates of $\boldsymbol{u}$ and $\dot{\boldsymbol{u}}$ at the nth ensemble, respectively. RMSE is defined as $RMSE(\boldsymbol{u}) = \sqrt{\frac{1}{N} \sum_{n=1}^{N} \|\boldsymbol{u}_n - \boldsymbol{u}\|^2}$ for the position and $RMSE(\dot{\boldsymbol{u}}) = \sqrt{\frac{1}{N} \sum_{n=1}^{N} \|\dot{\boldsymbol{u}}_n - \dot{\boldsymbol{u}}\|^2}$ for the velocity, where $N = 5000$ is the total number of ensemble runs.

The localisation scenario in Zhu and Feng[13] is used. The scenario has an array of five sensors; their positions and velocities are listed in Table 1. The TDOA and FDOA measurements are generated by adding zero-mean Gaussian noises with the covariance matrix $\boldsymbol{Q} = \mathrm{diag}(\delta^2 \boldsymbol{Q}_r, 0.1\delta^2 \boldsymbol{Q}_r)$, where $\boldsymbol{Q}_r = 0.5(\boldsymbol{I} + \boldsymbol{I}^T \boldsymbol{I})$, and $\boldsymbol{I}$ is a unit array. In this simulation, we consider near- and far-field scenarios in the moving source localisation. The estimation bias and accuracy of the source are investigated with the increase in TDOA and FDOA measurement noise.

Near-field scenario

In the near-field case, the true position and velocity of the target are $\boldsymbol{u} = [285, 320, 275]^T \mathrm{m}$ and $\dot{\boldsymbol{u}} = [-20, 15, 40]^T \mathrm{m \cdot s^{-1}}$, respectively.[13] The noise level δ^2 varies from -30 in log scale to 40 in log scale. We set the original interval vectors to $[\boldsymbol{u}] = [[-500, 500], [-500, 500], [-500, 500]]^T \mathrm{m}$ and $[\dot{\boldsymbol{u}}] = [[-50, 50], [-50, 50], [-50, 50]]^T \mathrm{m \cdot s^{-1}}$.

Figure 1 shows that the estimation bias norm of the proposed method is significantly smaller than those of TSWLS, ML and CTLS, especially for high measurement noise levels.

Figure 2 plots the accuracy of the position and velocity estimates of TSWLS, ML, CTLS and the proposed method, in terms of the RMSE with increasing δ^2. The three methods can approach the CRLB at a low noise level. For the source position estimation, the threshold effect of the proposed method occurs at 28 dB, which is later than the others. In the velocity estimation, TSWLS, ML and CTLS also provide inaccurate estimates that are apparently earlier than that of the

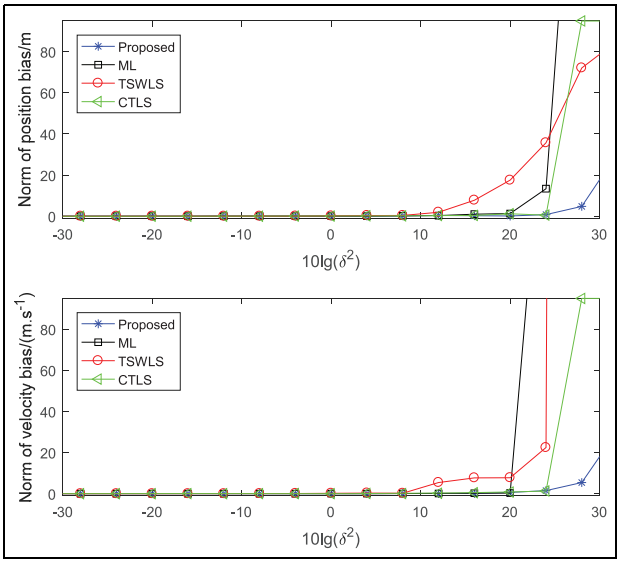

Figure 1. Comparison of the estimation bias of the proposed estimator with TSWLS and ML versus measurement error for target located at (280, 325, 275) m.

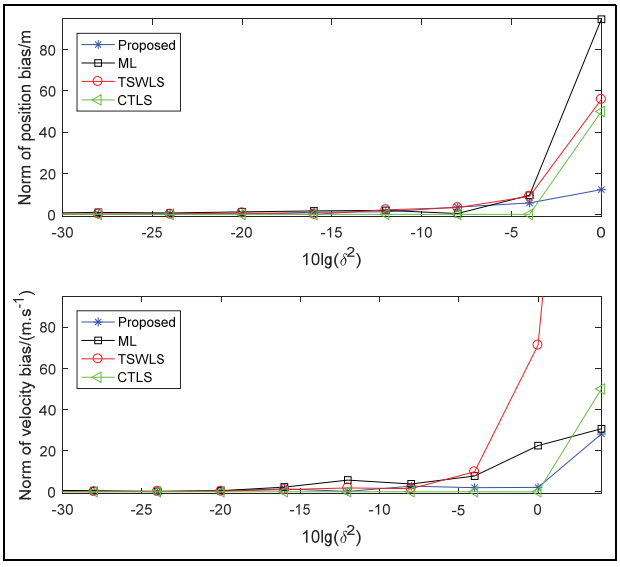

Figure 3. Comparison of the estimation bias of the proposed estimator with TSWLS and ML versus measurement error for target located at (1000, 1500, 2000) m.

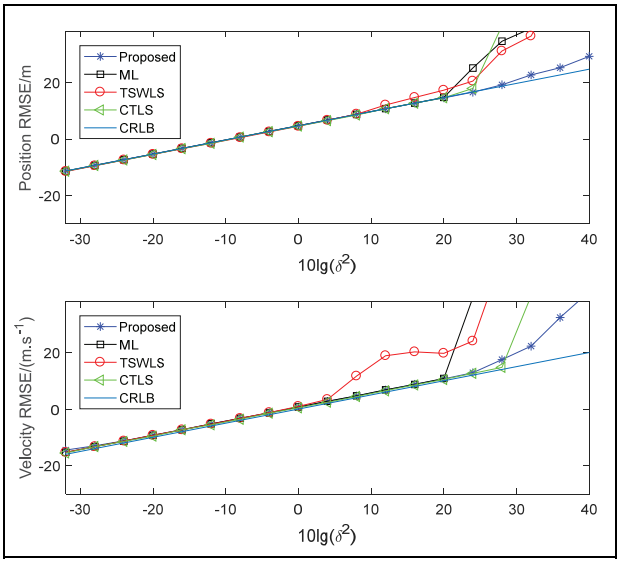

Figure 2. Comparison of RMSE of the proposed estimator with TSWLS, ML and the CRLB versus measurement error for target located at (280, 325, 275) m.

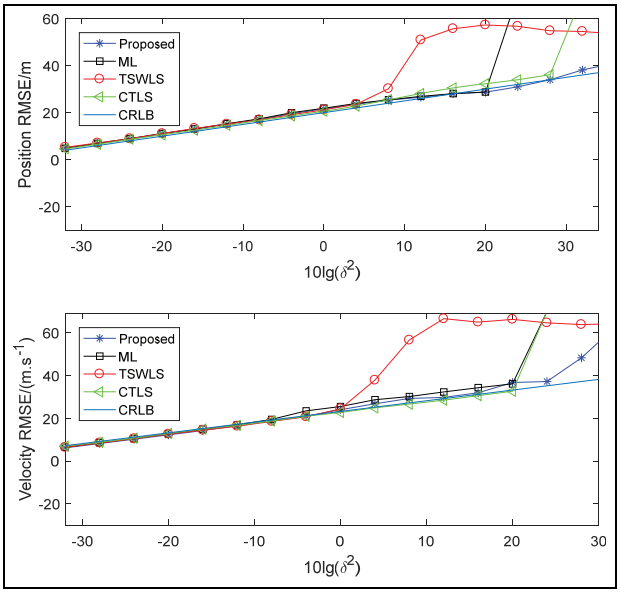

Figure 4. Comparison of RMSE of the proposed estimator with TSWLS, ML and the CRLB versus measurement error for target located at (1000, 1500, 2000) m.

proposed algorithm. For ML, it is very complicated to obtain initial estimation of position and velocity when noise increases. Excessive noise affects the construction of the weight matrix in TSWLS and CTLS, resulting in a large deviation of the estimated value.

Far-field scenario

In the far-field case, we set the true target position $\boldsymbol{u} = [1000, 1500, 2000]^T$m and velocity $\dot{\boldsymbol{u}} = [-20, 15, 40]^T$m $\cdot$ s^{-1},[10] whereas the noise level δ^2 varies from -30 in log scale to 20 in log scale. The original interval vectors of the moving source position and velocity are $[\boldsymbol{u}] = [[-3000, 3000], [-3000, 3000], [-3000, 3000]]^T$m and $[\dot{\boldsymbol{u}}] = [[-50, 50], [-50, 50], [-50, 50]]^T$m $\cdot$ s^{-1}, respectively.

Figure 3 depicts that the estimation bias norms of the four methods in the far-field case are more unstable than those in the near-field case, but the location and velocity estimation biases of the proposed algorithm

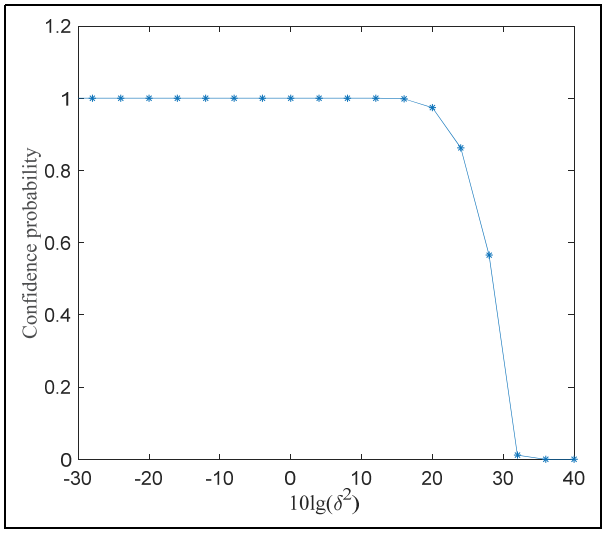

Figure 5. Confidence probability of the proposed algorithm.

are relatively small even at the high measurement noise level.

As shown in Figure 4, the accuracy of the position and velocity estimates of TSWLS, ML, CTLS and the proposed method also decrease in terms of RMSE with increasing δ^2 in the far-field case. The three methods can reach the CRLB at a low noise level, but their threshold effects occur earlier than those in the near-field case because the location can be uniquely evaluated to a single coordinate point when the source is near the sensors where the wavefront is curved.[24,25] However, if the target is far from the sensors, the methods ignore the curvature of the wavefront. In the source position estimation, the threshold effect of the proposed method occurs at 25 dB, which is also later than the others. For the velocity estimation, the performance of the proposed algorithm is similar to that of the location estimation.

Confidence probability

For source location and velocity estimations, the proposed method can not only provide a point estimate, but also the confidence interval. When the simulation scenario and parameter settings are consistent with the near-field case, the algorithm provides the interval vector of the position and velocity of the source, that is., $[\boldsymbol{u}]$ and $[\dot{\boldsymbol{u}}]$, where they include their true values. Confidence probability measures the probability that the interval vector contains the true solution and is defined as $\frac{n}{N}$, where N is the total number of independent trials, and n is the number of trials whose interval vectors include the true position and velocity of the source. As shown in Figure 5, the proposed algorithm can guarantee that the true source position and velocity are contained in the interval vector when δ^2 is lower than 20 in log scale.

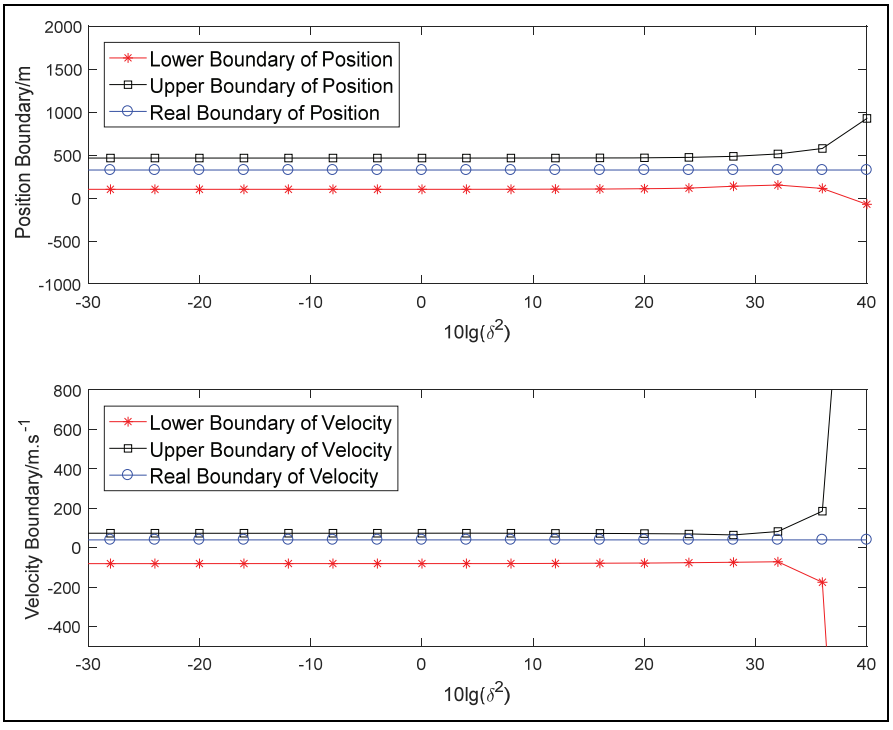

Figure 6. Estimation boundary of position and velocity of the proposed estimator.

Table 2. The computational complexity of four algorithms.

Algorithm	Multiplication times	Average times(s)
Proposed	$O_{((N_{iter}+1)N^2)}$	3.9×10^{-3}
ML	$O_{((N_{iter}+1)N^2)}$	4.9×10^{-3}
TSWLS	$O_{(N^3)}$	2×10^{-3}
CTLS	$O_{(N^3)}$	4.5×10^{-2}

ML: maximum likelihood; TSWLS: two-step weight least-square; CTLS: constrained total least-square.

The specific boundaries of the location and velocity estimates of the proposed method in the X-axis are also shown in Figure 6. When δ^2 is lower than 30 in log scale, the boundaries of the interval vector also remain the same. This result indicates that the proposed algorithm can provide a reliable range of position and velocity estimates at low and moderate noise levels.

Computational complexity

In this paper, the multiplicative times of four algorithms are used as a measure of computational complexity. As shown in Table 2, TSWLS and CTLS have the same computational complexity $O_{(N^3)}$. In contrast, the computational complexity of the proposed algorithm and ML algorithm are $O_{((N_{iter}+1)N^2)}$, where N_{iter} is the number of iterations. After $N = 5000$ independent simulation experiments, the average running time of the proposed method, ML, TSWLS and CTLS are 3.9×10^{-3}s, 4.9×10^{-3}s, 2×10^{-3}s and 4.5×10^{-2}s, respectively. The results show that the proposed method can reduce computation complexity in comparison with the traditional ML estimator and CTLS. Furthermore, the proposed method provides a more complex solution compared with TSWLS, but it is superior in accuracy performance.

Conclusion

In this study, we consider the problem of estimating a moving source using the TDOA-FDOA measurements obtained from multiple sensors based on the bounded error framework. By combining interval analysis with a bi-iterative strategy, we develop an efficient method that alternately calculates the source position and velocity interval vectors that enclose the true values. Simulation results show that the algorithm has superior performance over other methods and approaches the CRLB at a sufficiently high noise level.

Acknowledgements

The authors give their thanks to editors and the anonymous reviewers for the valuable comments and suggestions.

Declaration of conflicting interests

The author(s) declared no potential conflicts of interest with respect to the research, authorship, and/or publication of this article.

Funding

The author(s) disclosed receipt of the following financial support for the research, authorship, and/or publication of this article: All the authors appreciate the supports from the National Natural Science Foundation of China, No.61702228, 61803183, 61304264, the Natural Science Foundation of Jiangsu Province, No.BK20170198, BK20180591, Jiangsu Planned Projects for Postdoctoral Research Funds, No.1601012A, the Fundamental Research Funds for the Central Universities, No.JUSRP1805XNC and the 111 Project (B12018), The Open Fund of Key Laboratory of Dynamic Cognitive System of Electromagnetic Spectrum Space of Ministry of Industry and Information Technology (Grant No. KF20202104).

ORCID iD

Ningning Qin https://orcid.org/0000-0002-1119-7334

References

1. Malanowski M and Kulpa K. Two methods for target localization in multistatic massive radar. *IEEE Trans Aerospac Electr Syst* 2012; 48(1): 572–580.
2. Ho KC and Chan YT. Geolocation of a known altitude object from TDOA and FDOA measurements. *IEEE Trans Aerosp Electron Syst* 1997; 33(3): 770–783.
3. Cao Y, Peng L, Li J, et al. A new iterative algorithm for geolocating a known altitude target using TDOA and FDOA measurements in the presence of satellite location uncertainty. *Chin J Aeronaut* 2015; 5: 1510–1518.
4. Patwari N, Ash JN, Kyperountas S, et al. Locating the nodes: cooperative localization in wireless sensor networks. *IEEE Signal Pr Mag* 2005; 22(4): 54–69.
5. Foy WH. Position-location solution by Taylor-series estimation. *IEEE Trans Aerosp Electron Syst* 1976; 12(2): 187–194.
6. Lu XN and Ho KC. Taylor-series technique for moving source localization in the presence of sensor location errors. In: *IEEE international symposium on circuits and systems (ISCAS'06)*, Island of Kos, 21–24 May 2006, pp.1075–1078. New York: IEEE.
7. Noroozi A, Oveis AH, Hosseini SM, et al. Improved algebraic solution for source localization from TDOA and FDOA measurements. *IEEE Wirel Commun Lett* 2018; 7(3): 352–355.
8. Ho KC and Xu W. An accurate algebraic solution for moving source location using TDOA and FDOA measurements. *IEEE T Signal Pr* 2004; 52(9): 2453–2463.
9. Ho KC, Lu X and Kovavisaruch L. Source localization using TDOA and FDOA measurements in the presence of receiver location errors: analysis and solution. *IEEE T Signal Pr* 2007; 55(2): 684–696.

10. Zou Y and Liu H. An iterative method for moving target localization using TDOA and FDOA measurements. *IEEE Access* 2018; 6: 2746–2754.
11. Zhou L, Zhu W and Luo J. Direct positioning maximum likelihood estimator using TDOA and FDOA for coherent short-pulse radar. *IET Radar Sonar Navigat* 2017; 11: 1505–1511.
12. Othman MAK and Capolino F. Theory of exceptional points of degeneracy in uniform coupled waveguides and balance of gain and loss. *IEEE T Antenna Propag* 2017; 65(10): 5289–5302.
13. Zhu G and Feng D. Bi-iterative method for moving source localisation using TDOA and FDOA measurements. *Electr Lett* 2015; 51(1): 8–10.
14. Zhu G, Feng D, Xie H, et al. An approximately efficient Bi-iterative method for source position and velocity estimation using TDOA and FDOA measurements. *Signal Pr* 2016; 125: 110–121.
15. Abdallah F, Gning A and Bonnifait P. Box particle filtering for nonlinear state estimation using interval analysis. *Automatica* 2008(3)44: 807–815.
16. Jaulin L and Walter E. Set inversion via interval analysis for nonlinear bounded-error estimation. *Automatica* 1993; 29(4): 1053–1064.
17. Iwi G, Millard RK and Palmer AM. Bootstrap resampling: a powerful method of assessing confidence intervals for doses from experimental data. *Nucl Med Commun* 2000; 44: 55–62.
18. Jaulin L, Kieffer M, Didrit O, et al. Interval analysis. In: L Jaulin, M Kieffer, O Didrit, et al. (eds) *Applied interval analysis*. New York: Springer, 2001, pp.11–43.
19. Shen Z and Zhu Y. An interval version of shubert's iterative method for the localization of the global maximum. *Computing* 1987; 38: 275–280.
20. Liu Z, Hu D and Zhao Y. A bias compensation method for distributed moving source localization using TDOA and FDOA with sensor location errors. *Sensors* 2018; 18: 3747–3762.
21. Chen X, Wang D, Yin J, et al. Performance analysis and dimension-reduction Taylor series algorithms for locating multiple disjoint sources based on TDOA under synchronization clock bias. *IEEE Access* 2018; 6: 48489–48509.
22. Yang L and Ho KC. Alleviating sensor position error in source localization using calibration emitters at inaccurate locations. *IEEE T Signal Pr* 2010; 58(1): 67–83.
23. Zhang L, Wang D and Yu H. A ML Method for TDOA and FDOA localization in the presence of receiver and calibration source location errors. In: *International conference on information and communications technologies (ICT 2014)*, Nanjing, China, 15–17 May 2014, pp.1–5. New York: IEEE.
24. Wang Y and Ho KC. Unified near-field and far-field localization for AOA and hybrid AOA-TDOA positionings. *IEEE T Wirel Commun* 2017; 17(2): 1242–1254.
25. Sun Y, Ho KC and Wan Q. Solution and analysis of TDOA localization of a near or distant source in closed-form. *IEEE T Signal Pr* 2019; 67(2): 320–335.